EPJ Appl. Metamat. **6**, 15 (2019)

https://doi.org/10.1051/epjam/2019008

EPJ Applied Metamaterials

Available online at:
epjam.edp-open.org

Metamaterials Research and Development in China

REVIEW OPEN ACCESS

Recent developments of metamaterials/metasurfaces for RCS reduction

Ya Fan[1,*], Jiafu Wang[1], Xinmin Fu[1], Yongfeng Li[1], Yongqiang Pang[2], Lin Zheng[1], Mingbao Yan[1], Jieqiu Zhang[1], and Shaobo Qu[1]

[1] Basic of Sciences, Air Force Engineering University, Xi'an, Shaanxi 710051, PR China
[2] School of Electronics and Information Engineering, Xi'an Jiaotong University, Xi'an, Shaanxi 710049, PR China

Received: 25 October 2018 / Accepted: 29 January 2019

Abstract. In this paper, recent developments of metamaterials and metasurfaces for RCS reduction are reviewed, including basic theory, working principle, design formula, and experimental verification. Super-thin cloaks mediated by metasurfaces can cloak objects with minor impacts on the original electromagnetic field distribution. RCS reduction can be achieved by reconfiguring scattering patterns using coding metasurfaces. Novel radar absorbing materials can be devised based on field enhancements of metamaterials. When combined with conventional radar absorbing materials, metamaterials can expand the bandwidth, enlarge the angular range, or reduce the weight. Future tendency and major challenges are also summarized.

Keywords: Metamaterials and metasurfaces / RCS reduction / cloaks / scattering manipulation / microwave absorbers

1 Introduction

Left-handed material with negative permittivity and negative permeability is a typical type of metamaterial, which possesses many novel physical characteristics, such as negative phase shift, negative reflection/refraction, inverse Doppler effect, and backward Cerenkov radiations [1]. However, due to the lack of such materials in nature, this concept did not attract much attention until the experimental verifications of negative permittivity and negative permeability at microwave frequency using artificial structures by Pendry et al. [2,3], respectively. In 2001, Smith and coworker's firstly observed negative permittivity and permeability simultaneously in the combination of metal wires and split ring resonators (SRRs) [4]. Since then, metamaterials have achieved huge developments and been widely applied in areas of mechanics [5–7], acoustics [8,9], optics [10,11], and microwave engineering [12]. As an important branch, planar metamaterial constructed by a two-dimensional array of subwavelength structures is called metasurfaces [13]. Owing to subwavelength dimensions and flexible arrangements, the effective surface parameters of metasurfaces can be designed to be inhomogeneous and anisotropic [14]. On the basis for transformation optics and physical principles, this unique ability to flexible design makes metamaterials and metasurfaces very efficient in controlling the electromagnetic (EM) waves. Hence, lots of unusual and fantastic phenomena that cannot generate by conventional media have been achieved utilizing metamaterials or metasurfaces, such as negative refraction [15–17], super-resolution imaging [18], invisible cloaking [19–21], microwave and optical black holes [22,23], perfect absorption [24–26], anomalous reflection [13,27], asymmetric transmissions [28–30], optical and microwave vortex [31–33], photonic spin Hall effect [34], and polarization rotation [35–37], etc.

Recently, applications of metamaterials and metasurfaces for low-observation platforms have attracted enormous interests due to their unusual properties [38–48]. Without considering signal distortion, these radar cross section (RCS) reduction technologies can be generally classified into three categories according to respective working principle: metamaterials/metasurfaces for electromagnetic wave (EMW) cloaking, scattering, and absorbing. In 2006, Pendry et al. and Leonhardt proposed the transformation optic (TO) theory and an EM cloak that could render a given volume invisible to EM waves, which also provide an efficient way to control the propagating direction, polarization state, amplitude, and phase of EM waves [49,50]. The concept of the invisible cloak realized using the TO theory was later verified by experiments in the microwave frequency [51]. Then, arbitrarily shaped cloaks have been proposed to cloak

* e-mail: albert_fan028@foxmail.com

obstacles with regular and irregular shapes [52–54]. Such cloaks were improved by using layered structures of homogeneous isotropic/anisotropic materials to facilitate their practical design and fabrication. Meanwhile, researchers started to explore other methods for EM cloakings. Alu and Engheta [19] attempted to realize plasmonic cloaks based on scattering cancellation, while Wang et al. proposed another scheme based on transmission-line networks. For instance, two approaches for EM cloaking were experimentally verified by using lumped inductors and capacitors and metallic transmission-lines [55,56].

EM scattering is another efficient technology for RCS reduction without absorbing the EMW energy [38–42]. Macroscopically speaking, the main idea is to deflect or distribute the incident EMWs in all directions so as to make the object undetectable. Traditionally, this was always achieved by adopting angular shapes and irregular surface to reflect incident waves into the non-threatening angular domain so as to increase the survivability against radar detection. However, as mentioned above, subwavelength resonators of metasurface can provide a flexible way to reshape the wave-front by tailoring their dimensions, converting the polarization state [57] or adjusting their geometric positions [58]. Then, by artificially arranging the various resonators in a specific or random order, the constructed phase metasurfaces can show excellent properties for anomalous EMW scatterings. As an important milestone, in 2011, the general Snell's law of reflection and refraction was proposed and verified by introducing several abrupt phase shifts on a metasurface [59], resulting in a phase gradient that could be used to manipulate the wave-fronts of lights. Since then, phase metasurfaces have experienced rapid development, producing many interesting works for RCS reduction. In 2012, an appropriate gradient phase metasurface was used to couple spatially propagating waves into surface waves with high efficiency, the energy of which was tightly bounded on the surface [60]. Owing to the characteristic features of field enhancement and wavelength compression, this method for surface waves generating was further adopted to enhance the absorptivity and reduce the thickness of traditional absorbing materials. In 2014, Giovampaola and Engheta [61] proposed the concept of "digital metamaterials", which makes use of appropriate spatial mixtures of "metamaterial bits" to construct elemental "metamaterial bytes" with desired effective medium parameters [62–64]. In the same year, from the viewpoint of information process, Cui et al. introduced the concepts of coding, digital, and programmable metasurfaces [65]. As an example of their works, 1-bit coding metasurface was constructed by a sequence of binary coding particles "0" and "1", which correspond to "0" and "π" phase responses, respectively. For an alternative 1-bit code sequence, the backward RCS of the metasurface turns out to be greatly decreased due to the diffusion effect. Actually, the incident waves can be further scattered into more directions, if each coding bit contains more phase states. Moreover, the far-field scattering pattern of metallic objects can be efficiently controlled by the use of coding phased metasurface, which opens up a new perspective for field reconfiguration in the microwave regime [66–68].

As known to all, one of the mainstream approaches for EM absorber designs is to use Salisbury screens [69]. These absorbers are always constructed out of a resistive sheet located about a quarter wavelength away from an equal-sized perfect electric conductor (PEC). For seeking other routes for EMW absorbing, a high performance ultra-thin absorber was introduced by Engheta [70] with the use of high impedance metasurfaces. Instead of a quarter wave away from the PEC, the high impedance surface was used just next to the resistive sheet to realize a PMC plane and successfully fulfilled the required phase difference for field cancellation. Then in 2003, Kern and Werner [71] presented a novel approach for an ultra-thin absorber utilizing a GA-optimized metallic pattern printed on a very thin dielectric material backed by the PEC. The metallic pattern was a lossy screen, which could significantly absorb the EM energy by resonances. A one-layer ultra-thin metasurface absorber was then proposed and demonstrated by Mosallaei and Sarabandi [72]. The absorber was composed of a periodic square patch array etched on a dielectric substrate backed by a metal sheet. Due to strong resonances and a good impedance matching with the free space, the square patches were coupled to each other through lossy dielectric materials representing lumped resistors. On the basis of this concept, varied metallic pattern with different dimensions is applied to expand the absorbing bandwidth by merging multiple resonant frequencies [73–75]. In this review, from three mentioned respects for RCS reduction, we have introduced several novel approaches based on metasurface and metamaterial for cloaking, scattering, and absorbing by our group researchers in recent years.

2 Metasurfaces for EM cloaking

2.1 Super-thin cloak mediated by spoof surface plasmons

Bandwidth extension, thickness reduction, and bigger cloaking region are now the three key issues of cloaks. Nevertheless, to enlarge the cloaking region, it is of great importance to introduce more complicated theoretical analysis as well as complex designs. Cloaks based on the TO theory exhibit quite broad bandwidth for cloaking, but suffer from bulky volume and large thickness, comparable to the radius of cloaked object. In reference [76], Wang et al. of our group reported several novel super-thin spoof surface plasmon (SSP) cloaks for large objects. SSP is the counterpart of surface plasmon polariton (SPP) in microwave regime. Due to strong field confinement, SPPs and SSPs are capable of modulating EM waves at subwavelength scales. Coordinate transformations are applied to analyze a microwave SSP-supporting system, an interface between air and microwave magnetic metamaterial. Figure 1 gives an 8.2 GHz cloak implemented using SRRs. Thickness of the cloak is less than 1/50 the cloaked diameter. Since the SSP fields are the highly bounded around the cloaked object, such cloaks have shown lots of promising applications in areas of weak wave detection and high-sensitivity sensing. Then, inspired by

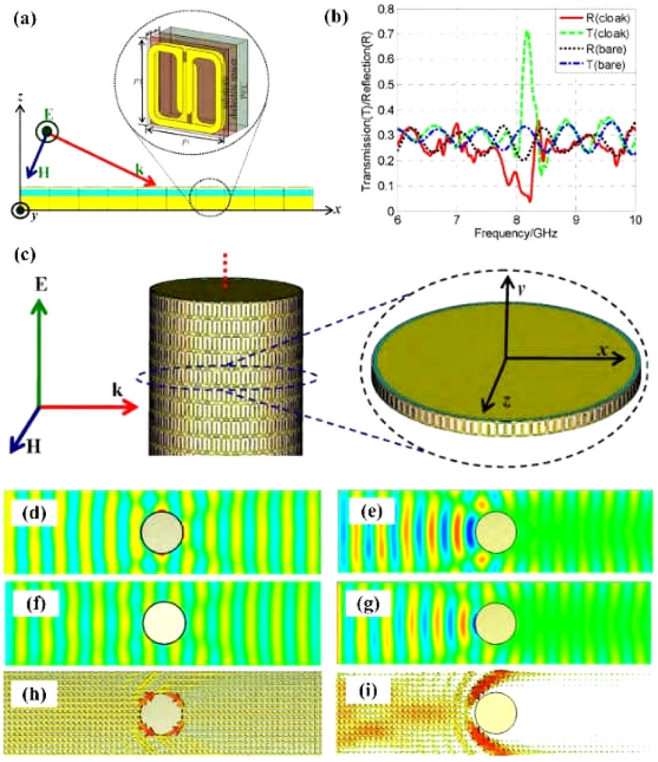

Fig. 1. (a) The schematic diagram of unit cell, (b) transmission/reflection comparisons with and without the cloaking, (c) implementation of a super-thin cloak, (d–i) the electric field, magnetic field, and power flow distributions at 8.2 GHz on x-o-z plane with (the left panel) and without (the right panel) the cloaking. From reference [76]. Reprinted with permission from Elsevier.

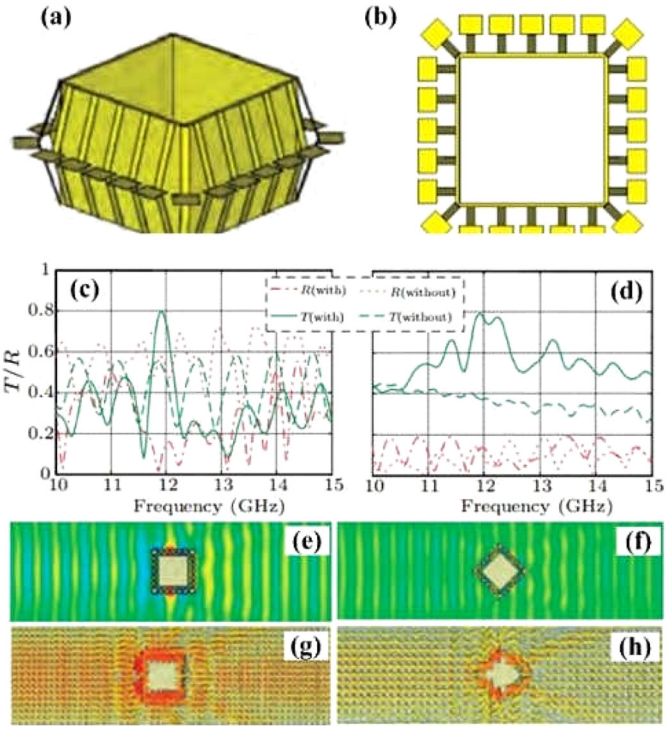

Fig. 2. (a, b) Perspective and top views of rectangular copper shell with GCW cloak, (c, d) transmission/reflection comparisons with and without cloak, (e–h) electric field snapshot and power flow at 11.9 GHz under side (the left panel) and edge (the right panel) incidences. From reference [77]. Reprinted with permission from IOP.

the concept of grating-coupled waveguide (GCW), another cylindrical EM cloak wrapped with evenly spaced elementary metallic structures [77] has been proposed and demonstrated by the same authors, as shown in Figure 2. The bulgy patches play the role of gratings to efficiently couple incident waves onto the attached metallic lines and then decoupled into the free space behind the cloaked obstacle. The metallic lines also play the role of waveguides to transfer incident energy to the back of the cloaked obstacle and keep the wave-front's shape by phase compensation. This kind of cloaks can be readily applied to cloak more complicated objects and is also quite easy to fabricate in practice.

2.2 Super-thin cloak based on microwave networks

To reduce the whole thickness of cloak, Wang et al. further proposed a new scheme to super-thin EM cloaks by means of microwave networks [78], as illustrated in Figure 3a. The unit resonator of the cloak is equivalent to a three-port microwave network. Under normal illumination, one of the three ports is aimed to receive EM waves, while the other two ports are adopted to transfer the received energy around the cloaked object and finally retransmitted into the shadowed region. As a result by this way, desirable but non-perfect cloaking effects can be obtained. A $\lambda/40$ thick cloak was presented for artificial and experimental demonstrations. The designed cloak is made of a number of interconnected metallic patches attached around the cloaked object. From Figure 3b, it should be noted that a normal transmission peak occurs at 3.63 GHz. Concluding from the field distributions given in Figure 3c,e,g at 3.63 GHz, we can see the amplitudes of electric/magnetic fields before and after propagating through the cylinder almost remain the same. More importantly, the phase-front shape is excellently kept after passing through the copper cylinder. Comparatively, strong reflection occurs on the case of the copper cylinder without the cloak. This can also be verified by obvious shadowed region phase-fronts are distorted in the back of the cylinder as depicted in Figure 3d,f,h. Owing to thin thickness and easy fabrication, the design method inspired from microwave network can exactly provide an alternative way to realize super-thin EM cloak.

2.3 Broadband unidirectional cloak based on flat metasurface focusing lenses

Then inspired by geometric optic theory, as shown in Figure 4, Li et al. of our group then proposed a thin unidirectional EM cloaks using transmitted

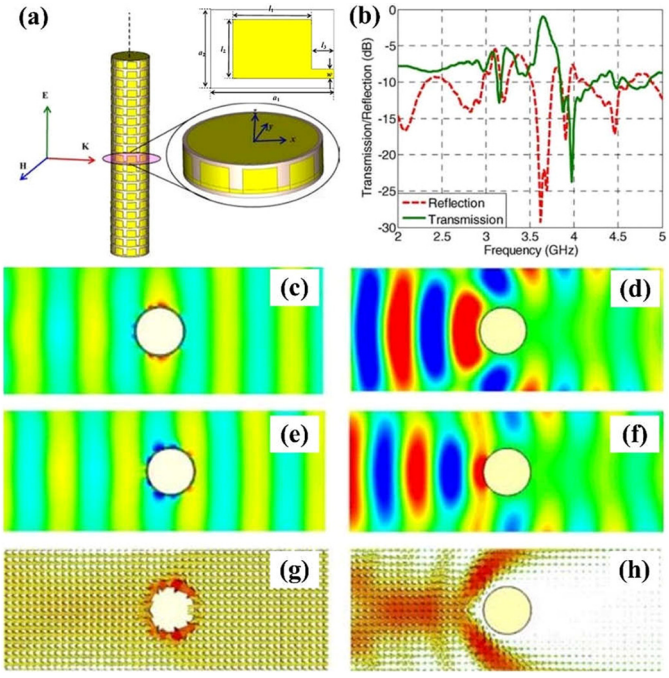

Fig. 3. (a) Copper cylinder enclosed by the designed cloak, (b) transmission and reflection for an infinitely long copper cylinder with cloak, (c–h) the electric field, magnetic field, and power flow distributions at 3.63 GHz on x-o-y plane with (the left panel) and without (the right panel) the cloak. From reference [78]. Reprinted with permission from IEEE.

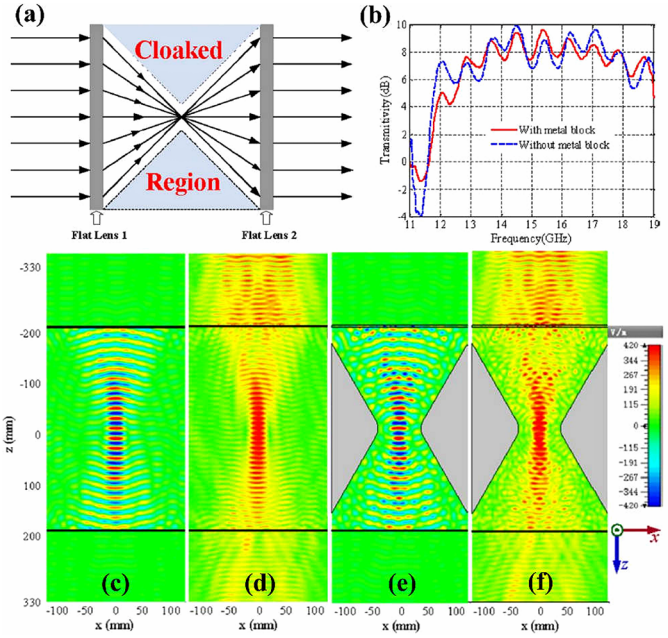

Fig. 4. (a) Principle diagram of the proposed unidirectional cloak, (b) the normal transmissions of the designed unidirectional cloak with and without the metal block, the simulated distributions of the E_x field and the amplitudes of the electric fields $|E|$ at 16 GHz on the x-o-z plane, (c, d) for cloak without triangle metallic blocks, (e, f) for cloak with triangle metallic blocks. From reference [79]. Reprinted with permission from IOP.

metasurfaces [79]. To this end, a flat focusing lens was firstly devised by elliptical SRRs, characterized by broadband and high cross-polarization conversion efficiency. Discrete transmitted phases are obtained by tailoring the width of split ring and rotating around the resonator's center. For compensating the phase difference caused by the wave path-difference, a nearly dispersionless parabolic phase profile is artificially distrusted on the metasurface. Two identical metasurface lenses were then used to construct the broadband unidirectional EM cloak. Under normal illumination, incident plane waves can be focused efficiently after passing through the front flat lens and then restored by the other one, avoiding the cloaked region. Due to broad bandwidth and small thickness, such cloaks designed by this way show potential applications in making electrically large objects invisible.

3 Phase metasurfaces for EMW scattering

Wave-front shaping is always realized by a gradual phase accumulated along the wave propagation path, which makes conventional optical devices surfer from bulky volume. To address this drawback, the concept of discontinuity abrupt phase changes achieved using an array of sub-wavelength resonators has been proposed and demonstrated for efficiently wave-front shaping under normal illumination. When the discrete phases are in common difference, such thin artificial surfaces are so called phase gradient metasurface (PGM). As indicated by the published works of metasurfaces, abrupt phase responses are always introduced by dimension tailoring, polarization state converting, and geometric position rotating of the resonators. By periodically or non-periodically arranging these resonators with different phase profile, the formed metasurfaces can exhibit low RCS performance within the specific frequency interval of interest.

3.1 Polarization independent phase gradient metasurface

Early in 2012, a perfect SSPP coupler based on PGM has been proposed and demonstrated by our group using SRRs [80]. Normally incident EM waves are coupled efficiently into SPPs bound to the surface of PGM, although this only takes place in a narrow bandwidth. Then, following the similar idea, Li et al. of our group proposed to achieve RCS reduction using two-dimensional PGMs [81]. Two physical principles (surface wave coupling and anomalous reflection) have been applied to achieve broadband and high-efficient RCS reduction. When the introduced phase gradient is larger than the wave vector k_0 in free space, the incident waves are efficiently absorbed and loss by dielectric material due to surface wave coupling. On the other hand, when it is less than k_0 within the corresponding frequency band, the incident waves are deflected to the non-threatening angular domain because of

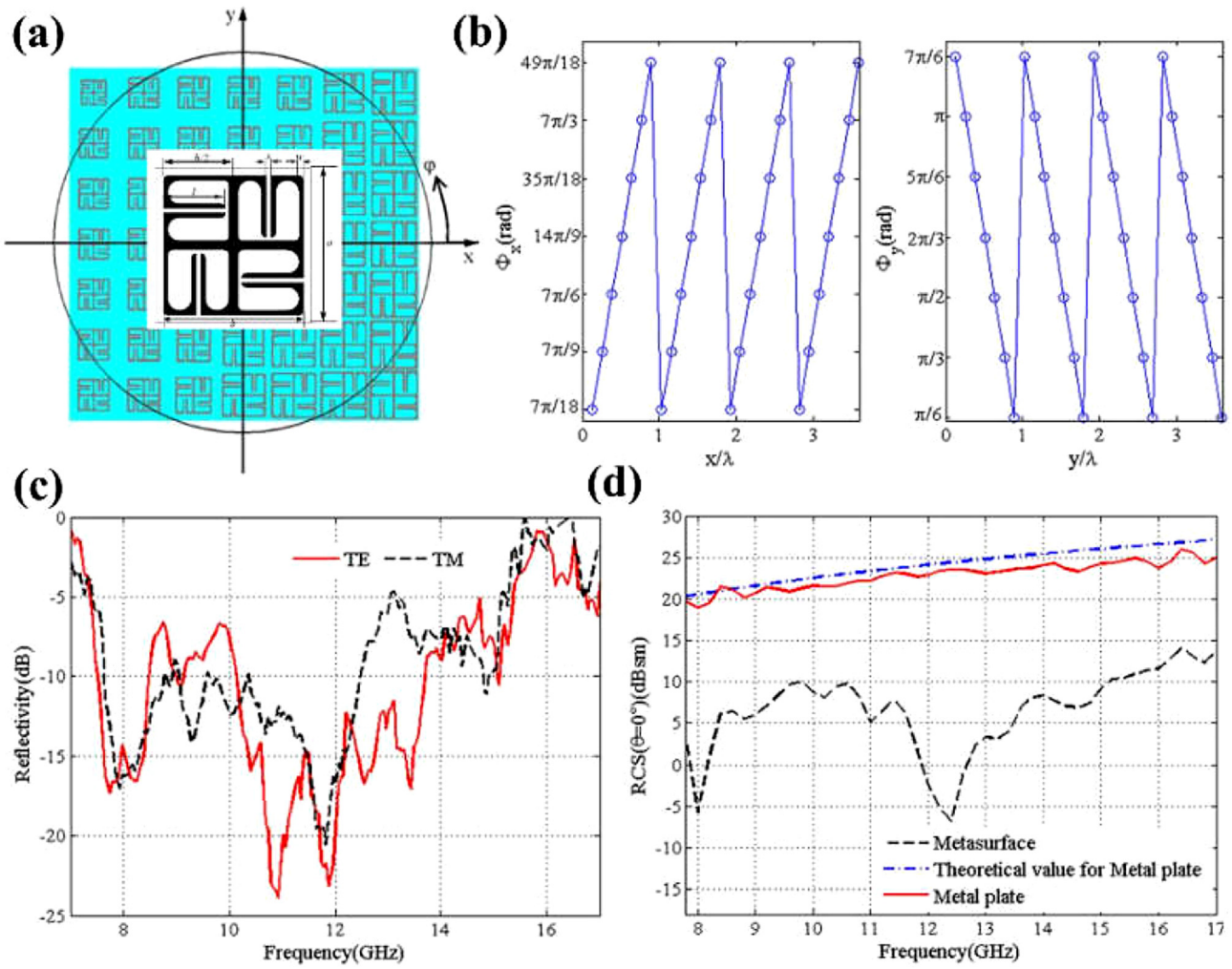

Fig. 5. (a) Super unit cell of 2D PGM, (b) phase profile of 2D PGM along two orthogonal in-plane directions at 7.7 GHz, (c, d) measured reflections and RCS versus frequency under normal incidence. From reference [81]. Reprinted with permission from AIP.

anomalous reflections. Consequently, owing to these two physical mechanisms, the RCS has been dramatically reduced in a wide frequency band. Since the adopted resonators are symmetric, such PGMs are polarization-insensitive. As the results given in Figure 5, the sub-array of the 2D PGM consists of a square combination of 7*7 subwavelength SRRs. Both the simulated and experimental results show that the proposed metasurface can realize wideband, polarization-insensitive, and high-efficient RCS reduction over the frequency range from 7.8 to 17.0 GHz.

3.2 Cross-polarized phase gradient metasurface for anomalous reflection

Additionally, polarization mismatching also greatly contributes to the goal of low-observation so as to be detected by other radars. Since polarization-insensitive PGMs usually require to tailor symmetric resonators to modulate phase of reflected and transmitted waves, the bandwidth is thus seriously limited by resonant characteristic of the symmetric resonator. To further extend the bandwidth for anomalous reflection, Chen et al. of our group have proposed an alternative method to expand the bandwidth of PGMs by means of merging multiple resonances [82–83] for polarization conversion. As shown in Figure 6, asymmetric structures are adopted as the fundamental element for realizing wideband deflection, which possess ultra-wideband linear polarization (LP) conversion. By tailoring their dimension parameters, rotating their geometric positions, and cross-polarized conversion, a constant phase gradient is formed by several chosen resonators in a wide frequency band under normal incidence. As the results indicate, the proposed PGM has been demonstrated to be capable of deflecting the incident wave and converting the LP state into its orthogonal one within the broad frequency band. The corresponding deflected angle can be theoretically calculated by the generalized Snell's law.

Subsequently, based on the polarization theory of EM waves that LP waves can be decomposed into left-handed circular polarization (LCP) and right-handed circular polarization (RCP) waves with equal amplitudes, Li et al. proposed to realize wideband polarization-insensitive anomalous reflection of LP waves by reflective PGMs

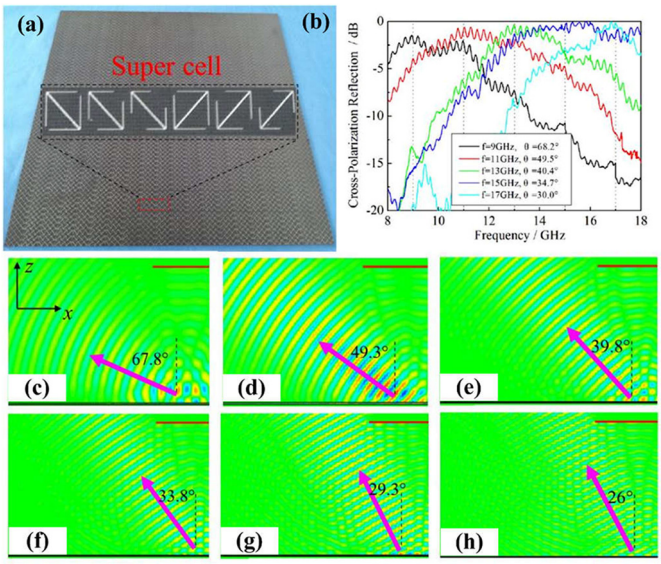

Fig. 6. (a) The photograph of fabricated sample and zoom-in view of super cell composed of six unit cells, (b) measured cross-polarized reflection versus frequency under normal x-polarized incidence, (c–h) the snapshots of electric field E_y for 9.0, 11.0, 13.0, 15.0, 17.0, and 19.0 GHz. From reference [82]. Reprinted with permission from AIP.

with dispersionless phase gradients for CP waves [84]. To ensure high-efficiency for anomalous reflection, near-unity co-polarization reflection is required. A metasurface reflector consists of N-shaped metallic resonators was then presented to realize wideband and highly efficient polarization-keeping reflection under LCP and RCP incidences, while cross-polarization reflection occurs on the metal plane. The polarization manipulation was controlled by different phase changes distributing along two in-plane directions due to the anisotropy of resonator. To this end, a reflective PGM was then designed to introduce a dispersionless phase gradient for CP waves. The phase gradient was introduced through rotating the resonators in-plane with a certain degree, as given in Figure 7. Due to opposite spin angular momentums of LCP and RCP waves, the in-plane phase gradient also exhibited opposite directions, respectively. As a result, the reflected LP waves were separated into two beams with opposite-signed reflection angles, which can be approximately calculated by the generalized Snell's law. Moreover, since the component LCP and RCP waves are irrelevant to polarization angles, the anomalous reflection is insensitive to the polarization angles of incident LP waves.

3.3 Coding metasurface for RCS reduction

Initially, coding metasurfaces [85] are aimed at digitalizing EM information of the metasurface by programming the amplitudes and phases of sub-wavelength resonators to control EM waves. After nearly a decade of development, this concept has been extended from microwave to terahertz frequencies [86], from isotropic to anisotropic, from reflection-type to transmission-type [87], from single-band to multi-band, and from spatial coding to time coding [88]. Initially, our group mainly focuses on the resonator optimization through genetic algorithm combined with some kinds of intelligent algorithm. Sui et al. developed this topology optimization method to design the fundamental element of metasurface [89]. On a properly thick dielectric substrate, the optimization area is divided into M*N smaller squares marked by "1" or "0". The element "1" indicates the unit area decorated with the resistive patch or metallic patch, while the element "0" means the one with nothing. In practical cases, the optimization goal usually is set as a multi-objective optimization problem including the desired frequency range, the absorption, the incident angle, etc. For a specific instance, a lightweight ultra-broadband wide-angle resistance frequency selective surface (FSS) absorber has been proposed and demonstrated, as shown in Figure 8.

Then, the authors have studied on encoding reflective phase information of subwavelength elements as a specific phase profile on the metasurfaces for further modulating the EM waves. Post-processed by the antenna array theory, this method has been verified to generate desired beams in the predesigned directions in far fields. For the goal of wideband but polarization independent RCS reduction without introducing multi-resonances, Sui et al. have designed a symmetric metallic resonators characterized with low Q-factor. These structures remain broad bandwidth but smooth phase changes as tailoring or scaling the geometric dimension. Two optimized elements with a 180° reflection phase difference are coded as "0" and "1", respectively. An example is given in Figure 9 to demonstrate the excellent diffusion performance of a 1-bit coding metasurface [90]. By arranging two coding elements randomly, incident EM waves have been scattered into numerous directions in the broad bandwidth of interest. The RCS has been dramatically reduced over 10 dB from 12 to 24 GHz, compared with an equal-sized PEC.

However, such symmetric coding resonators are lack of discordant resonant amplitudes, which take a negative influence on the efficiency for EM wave control. Additionally, it is necessary to find another way to further modulate the scattering patterns of coding metasurfaces, while specific number of beams, directions, even particular beam shape are required in more complicated low-RCS applications. To this end, coding element capable of co-polarization reflection under circularly polarized wave incidence should be a good candidate, because of their nearly unity amplitudes. Besides, owing to spin angular momenta carried by circularly polarized waves, arbitrary Pancharatnam–Berry (PB) phase change can be flexibly and simply obtained by rotating the coding element around the center, which is generally equal to the corresponding rotation angle. Since the Fourier transform relation between the coding pattern and its far-field radiation patterns, the convolution operations of multi far-field patterns in frequency can be processed by simply adding their coding patterns. Following a proof-of-principle demonstration of PB phase metasurface in reference [91], Feng et al. of our group have proposed a 2-bit coding metasurface for wideband RCS reduction by adding a 2D phase gradient with a random coding pattern [92]. Seen from the simulated far-field scattering

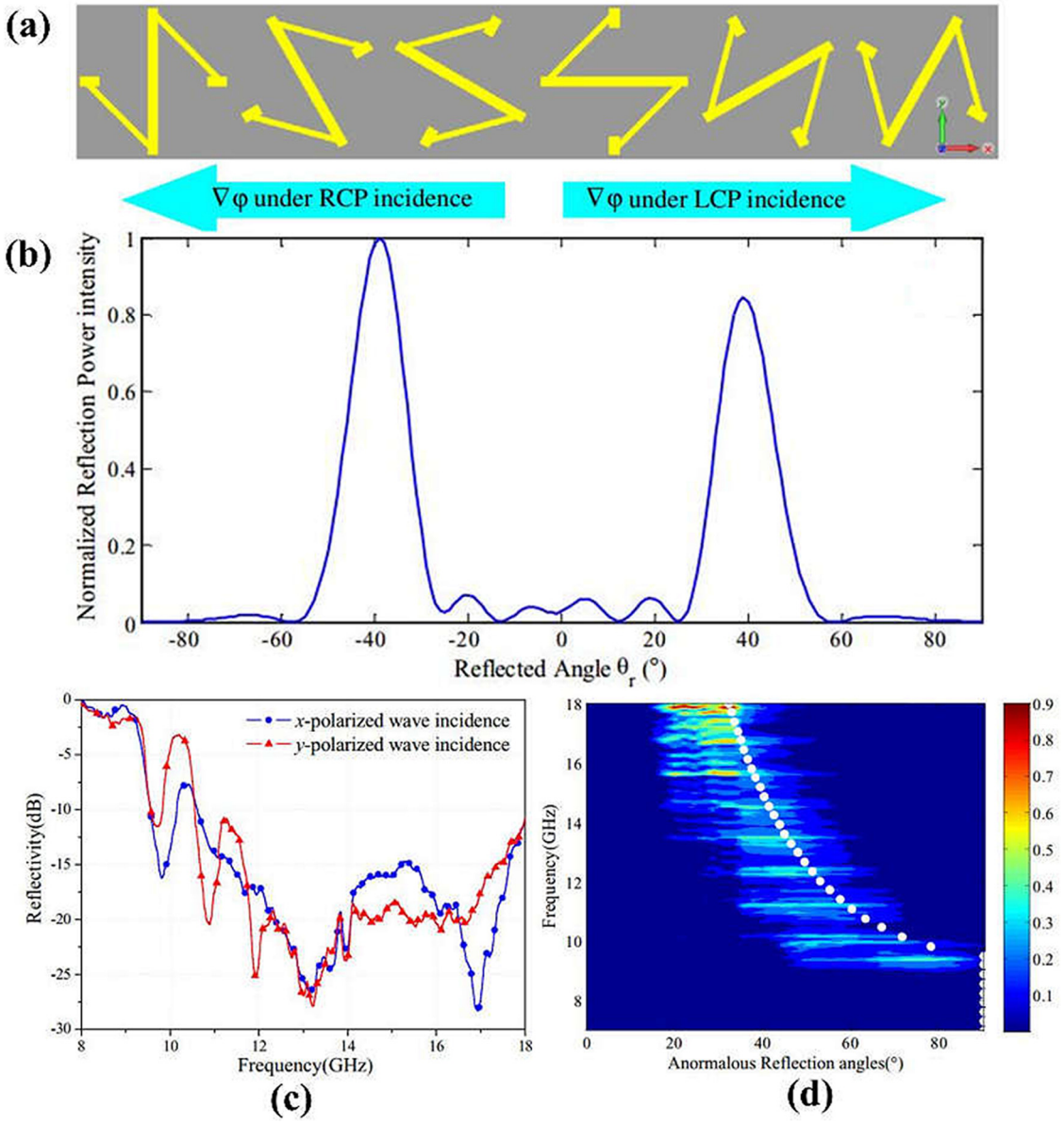

Fig. 7. (a) Schematic illustration of the super-unit of the designed PGM, (b) normalized reflection power intensity at 15 GHz, (c) measured reflection under linearly polarized incidence, (d) measured anomalous reflection angle spectra. From reference [84]. Reprinted with permission from IOP.

patterns in Figure 10e–h, under normal incident RCP and LCP waves, the reflected waves have achieved the diffusion scatterings by the random coding pattern and been deflected from the normal direction by 2D phase gradient. On the case of normally incident linearly polarized waves, the diffusion scatterings for decomposed RCP and LCP waves were reflected into two inverse directions with equal elevation and azimuth angles. To further verify the performance of RCS reduction, the authors measured the specular reflection and presented in Figure 10j, where it has been reduced more than 10 dB from 11.95 GHz to 18.36 GHz and 12.03 GHz to 18.48 GHz under normally incident x- and y-polarized waves.

4 Metamaterial/metasurface absorbers

4.1 Resistive metamaterial absorbers

With the supporting of screen printing technology, resistive film with strong Ohmic loss was employed to fabricate the metamaterial absorbers (MAs). As one of the important members of MAs, the resistive FSS proposed by Munk et al. is regarded as an alternative to design broadband absorber. Then, Sun et al. designed various absorbers utilizing resistive FSS [93]. Because the thickness of the plane MAs is much less than wavelength, the excitation of the EM resonance mode is single, resulting in narrow absorption band. Therefore, researchers tried to

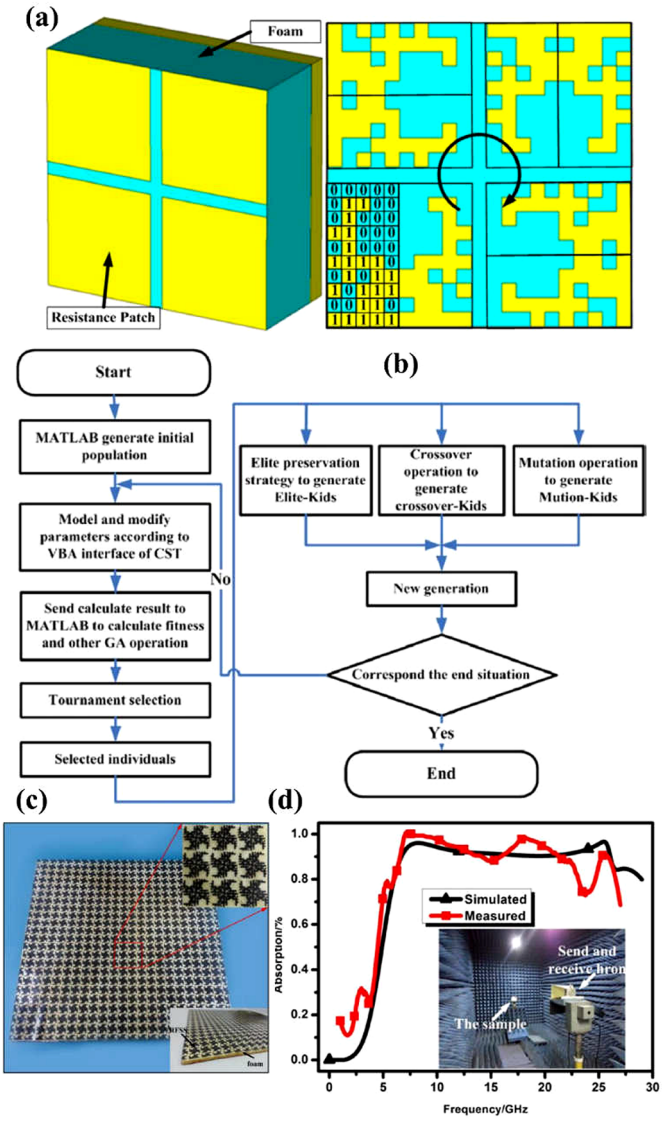

Fig. 8. (a) Code matrix of the FSSA structure by topology design, (b) flow chart of the optimization process, (c) the photograph of fabricated sample, (d) the absorption comparison between simulation and experiment. From reference [89]. Reprinted with permission from IOP.

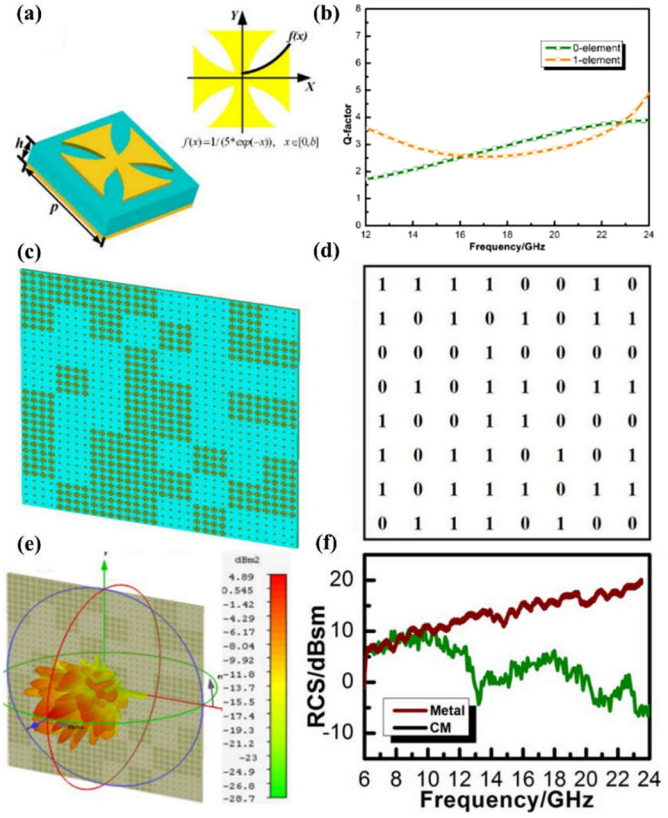

Fig. 9. (a) Schematic illustration of the unit cell, (b) the corresponding low Q-factor of elements "0" and "1", (c) the optimized configuration of CM, (d) corresponding random coding sequence, (e) the full wave simulation result of optimal CM, (d) the measured RCS comparison between CM and equal-size PEC. From reference [90]. Reprinted with permission from OSA.

extend 2D structure design to 3D. Shen et al. of our group proposed an absorber based on the standing-up resistive patch array [94], as shown in Figure 11. By rolling the resistive films into a cuboid-shaped box, the polarization-independent property can be obtained. Both the simulated and measured results of specular reflections indicate that the proposed absorber exhibits more than 90% absorption within the frequency range from 3.9 to 26.2 GHz. The ultra-wide absorption bandwidth mainly results from the multiple standing wave resonances excited by the stand-up resistive films and strong Ohmic losses. The areal density is as light as 0.062 g/cm^2. Furthermore, taking the example by the 3D origami structure, the authors then designed the metamaterials absorber with a folded standing-up resistive film lying on the metallic plane [95], as displayed in Figure 12. Compared with the conventional planar resistive FSS absorber, the designing scheme can easily fulfill good absorption for large incident angle. As verified by simulated and measured results, the proposed absorber can achieve the broadband and larger-incident angle absorption in the frequency band of 3.6–11.4 GHz, even when the incident angle is 75°. And the corresponding area density is only 0.023 g/cm^2.

4.2 Microwave absorber enhanced by metasurface incorporation

The conversional magnetic absorbing materials (MMs), profiting from large magnetic permeability and loss, had been widely employed to achieve broadband absorption in high frequency domain. However, it will suffer from large matching thickness, heavy weight, and narrow band when used in lower frequency. MA based on the configuration of metal resonator-dielectric sheet-metal backboard usually has narrow band due to its strong resonance. To overcome the deficiency, researchers proposed loading traditional absorbing materials to improve impedance matching and

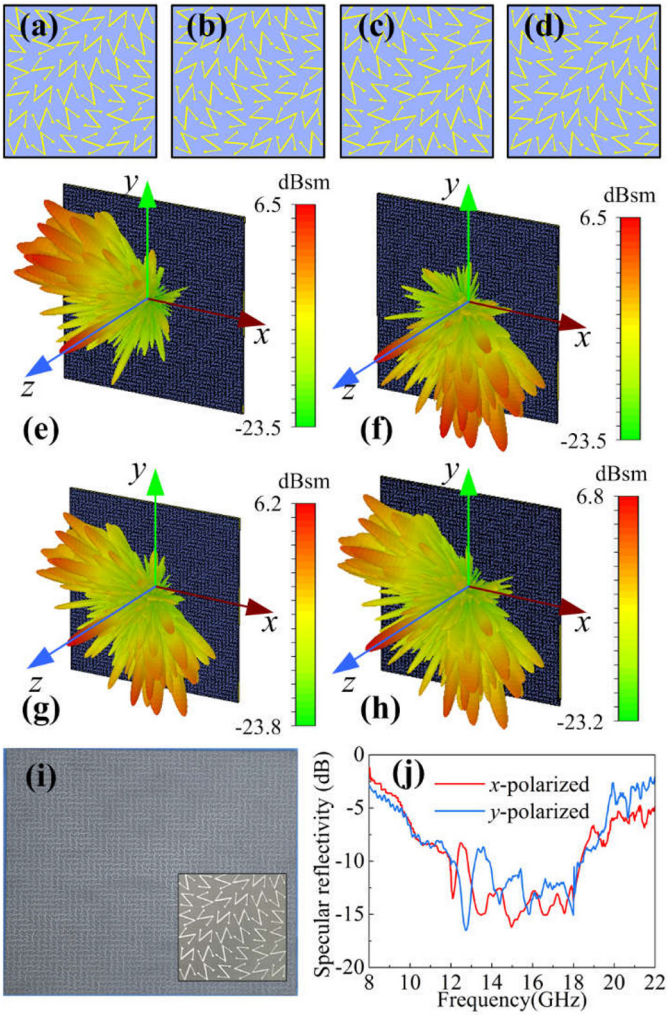

Fig. 10. (a–d) The unit cells of coding elements "00", "01", "10", and "11", (e–h) the simulate 3D far-field scattering pattern at 15 GHz under normal LCP, RCP, x-polarized and y-polarized incident waves, respectively, (i) the sample photograph where the inset is the detailed picture of coding element "00", (j) the specular reflections under normal x-polarized and y-polarized incident waves. From reference [92]. Reprinted with permission from IOP.

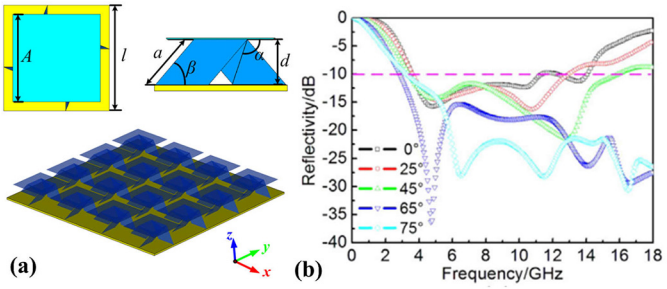

Fig. 12. MA based on standing-up resistive origami structure, (a) schematic structure, (b) simulated reflection spectra under the oblique incidences. From reference [95]. Reprinted with permission from IOP.

dispersion characteristics. Fan et al. of our group proposed a composite absorber (CA) consisting of the MM and ultra-thin PGM. The propagation distance of EMW in the MM can be enlarged by the anomalous refraction and reflection generated by the PGM, which makes the absorption property in low microwave frequency is improved [96]. As is shown in Figure 13, without changing the entire thickness and weight, the average specular reflection has been dropped down to lower than −10 dB from 2 GHz to 12 GHz, which indicates the absorptivity is more than 90%. In detail, by two physical mechanisms of EMW deflection and absorption, the absorbing property has been enhanced about 6 dB from 2 GHz to 3 GHz, decreased about 3 dB but still lower than −10 dB from 3 GHz to 4.8 GHz and improved near 3 dB in the 4.8–12 GHz frequency regime. The absorbing relative bandwidth is up to 143%. Meanwhile, water is served as a promising media due to its strong frequency dispersion at microwave frequencies. Thus, Pang et al. combined water with low-permittivity material (LPM) as the compounded dielectric substrate to design metamaterials absorbers [97]. Good absorbing performance can be obtained at the temperatures of interest. As an example given in Figure 14, the absorption efficiency was larger than 90% in the frequency range from 6.2 to 19 GHz at 20 °C. It is reasonable to believe that water can be a feasible candidate for designing other broadband thermal control absorbers.

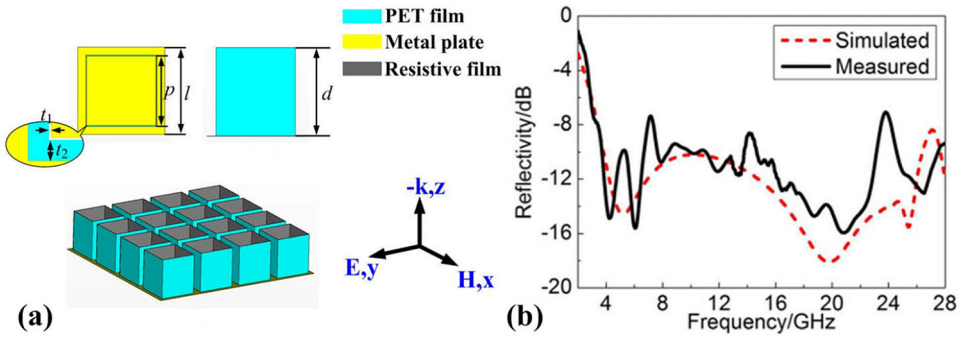

Fig. 11. MA based on standing-up resistive patch array, (a) schematic diagram, (b) the simulated and measured reflection under the normal incidence. From reference [94]. Reprinted with permission from AIP.

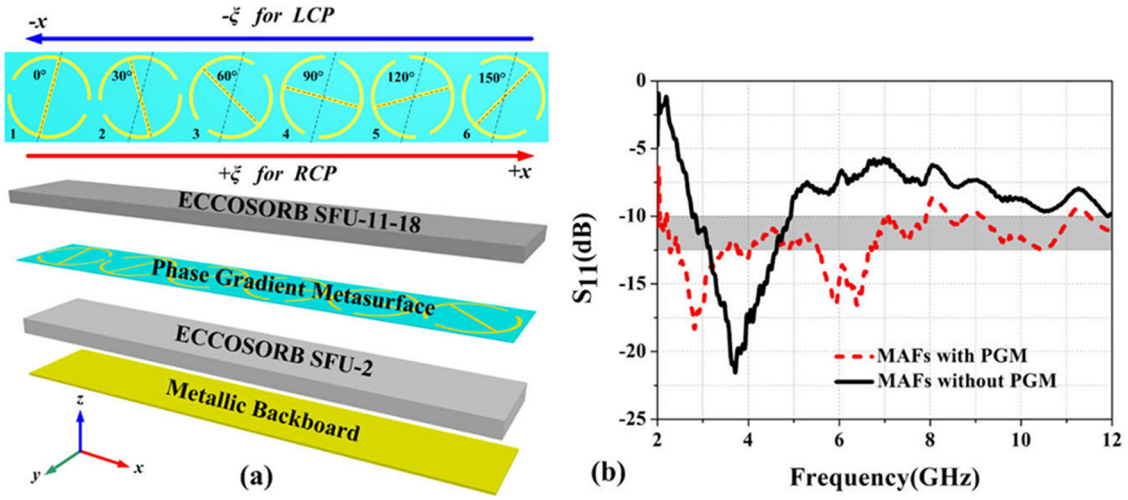

Fig. 13. (a) The diagram of the enhanced absorber, (b) the measured specular reflection S_{11} for the absorber enhanced with/without PGM. From reference [96]. Reprinted with permission from IOP.

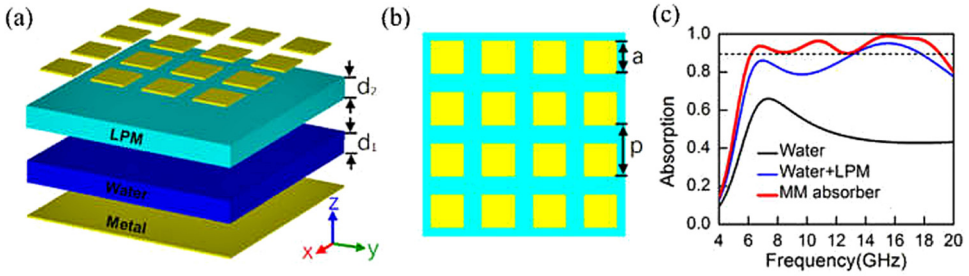

Fig. 14. (a) The diagram of water-substrate MM absorber, (b) the top view of it, (c) the absorption comparisons. From reference [97]. Reprinted with permission from AIP.

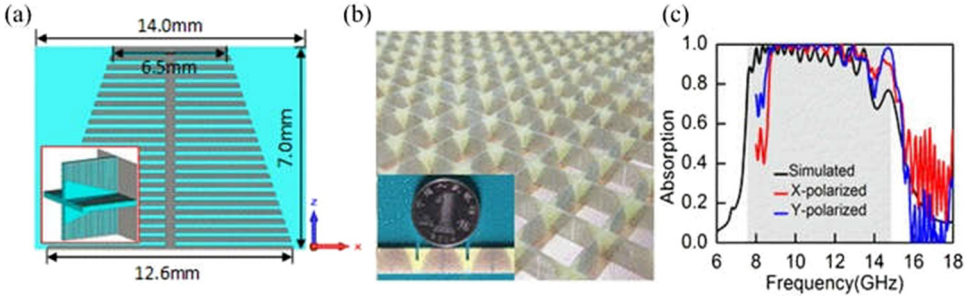

Fig. 15. (a) The unit of the absorber, (b) the fabricated absorber sample, (c) the comparison of the simulated and measured absorption. From reference [98]. Reprinted with permission from Nature.

4.3 Spoof surface plasmonic polaritons (SPPs) absorber

To investigate new approaches for energy absorbing, Pang et al. of our group proposed a concept to achieve customized broadband absorber using the spatial dispersion engineering of k-vector [98]. For this goal, SPPs characterized by controllable dispersion relations would be an ideal candidate to directly engineer the spatial dispersion of k-vector. Although SPPs naturally exist at optical frequencies, structured metamaterials have been demonstrated to excite and support spoof SPPs at microwave frequencies. Due to the field confinement within subwavelength dimensions of spoof SPPs, such metamaterials can achieve strong absorption by introducing proper losses. As shown in Figure 15, the authors adopted two orthogonally arranged corrugated plasmonic strips to create a broadband and frequency-selective spoof SPP absorber. The spatial dispersion relations are controlled by tailoring the length of the metallic lines. As an example, linearly varied lengths are applied to minimize the k-mismatching with the space wave. The absorption efficiencies for x- and y-polarized incidences are more than 90% within the frequency range in the gray region as

indicated in Figure 15c. It should be noted an important advantage of this concept is the easy process of material parameters and subsequent optimization. This concept can comparatively reduce the weight of absorber on the case of high absorption property, which also provides a new perspective for explaining many multiband and broadband MAs reported in previous works.

5 Summary and outlook

In conclusion, we have summarized the RCS reduction technologies based on metamaterials and metasurfaces and reviewed their developments in recent years. The review primarily concentrates on the design principle, phase change control, simulated, and experimental implementation. Without disturbing the original EM field distributions, we have demonstrated three kinds of EM cloaks for the goals of light weight, large cloaking area, and broad bandwidth. Utilizing phase changes caused by tailoring the dimensions, rotating their geometric positions of the resonators, and converting the polarization state of incident waves, metasurfaces designed with phase gradient profiles and random coding sequences have been verified to achieve excellent performances for broadband RCS reduction. From the presented examples, we can also see the powerful ability of phase metasurface to shape the near-filed distributions as well as tailor the far-field radiations in microwave regime. The paper finally reviews the developments of EMW absorbers improved by metamaterials or metasurfaces, including resistive metamaterials absorber, magnetic microwave absorber enhanced by PGM, and spoof surface polaritons (SSPs) absorber. As for various requirements in practical applications, although such metamaterials and metasurfaces have provided more flexible technical protocols, there are still several problems to solve in future work. One is to further miniaturize the dimensions of fundamental resonator into as small as or much smaller than deep sub-wavelength size. The second is to study new working principle for overcoming large thickness and bulk profile at low microwave frequencies. The last but the most important one is to investigate how to guarantee excellent RCS reduction performance of conformal metamaterials or metasurfaces.

This work was supported by National Natural Science Foundation of China (61771485, 61501497, 61501503, 61801509, 61671466, 61601507, 11504428, 61671467), National Key R&D Program of China (Grant No.2017YFA0700201).

References

1. V.G. Vexelago, The electrodynamics of substances with simultaneous negative values of ε and μ, Sov. Phys. Usp. **10**, 509 (1968)
2. J.B. Pendry, A.J. Holden, W.J. Stewart, I. Youngs, Extremely low frequency plasmons in metallic mesostructures, Phys. Rev. Lett. **76**, 4773 (1996)
3. J.B. Pendry, A.J. Holden, D.J. Robbins, W.J. Stewart, IEEE Trans. Microw. Theory Tech. **47**, 2075 (1999)
4. R.A. Shelby, D.R. Smith, S. Schultz, Experimental verification of a negative index of refraction, Science **292**, 5514 (2001)
5. J.N. Grima, L. Mizzi, K.M. Azzopardi, R. Gatt, Auxetic perforated mechanical metamaterials with randomly oriented cuts, Adv. Mater. **28**, 385 (2016)
6. B. Bar-On, F.G. Barth, P. Fratzl, Y. Politi, Multiscale structural gradients enhance the biomechanical functionality of the spider fang, Nat. Commun. **4**, 3894 (2013)
7. W. Jiang, H. Ma, M.D. Feng, L.L. Yan, J.F. Wang, J. Wang, S.B. Qu, Origami-inspired building block and parametric design for mechanical metamaterials, J. Phys. D: Appl. Phys. **49**, 315302 (2016)
8. Z.Y. Liu, X.X. Zhang, Y.W. Mao, Y.Y. Zhu, Z.Y. Yang, C.T. Chan, P. Sheng, Locally resonant sonic materials, Science **289**, 1734 (2000)
9. G.C. Ma, P. Sheng, Acoustic metamaterial: from local resonances to broad horizons, Sci. Adv. **2**, e1501595 (2016)
10. N.F. Yu, F. Capasso, Flat optics with designer metasurfaces, Science **13**, 139 (2014)
11. D. Lin, P.Y. Fan, E. Hasman, M.L. Brongersma, Dielectric gradient metasurface optical elements, Science **345**, 298 (2014)
12. T.S. Qiu, J.F. Wang, Y.F. Li, J. Wang, M.B. Yan, S.B. Qu, Magnetless circulator based on phase gradient metasurface, Acta Phys. Sin. **65**, 174101 (2016)
13. S.L. Sun, K.Y. Yang, C.M. Wang, T.K. Juan, W.T. Chen, C.Y. Lian, Q. He, S.Y. Xiao, W.T. Kung, G.Y. Guo, L. Zhou, D.P. Tsai, High-efficiency broadband anomalous reflection by gradient meta-surface, Nano Lett. **12**, 6223 (2012)
14. A.V. Kildishev, A. Boltasseva, V.M. Shalaev, Planar photonics with metasurfaces, Science **339**, 6125 (2013)
15. J. Valentine, S. Zhang, T. Zentgraf, E. Ulin-Avila, D.A. Genov, G. Bartal, X. Zhang, Three-dimensional optical metamaterial with a negative refractive index, Nature **455**, 7211 (2008)
16. D.R. Smith, N. Kroll, Negative refractive index in left-handed materials, Phys. Rev. Lett. **85**, 2933 (2000)
17. P.V. Parimi, W.T. Lu, P. Vodo, S. Sridhar, Photonic crystals: imaging by flat lens using negative refraction, Nature **426**, 6965 (2003)
18. Z. Jacob, L. Alekseyev, E. Narimanov, Optical hyperlens: far-field imaging beyond the diffraction limit, Opt. Express **14**, 8247 (2006)
19. A. Alu, N. Engheta, Achieving transparency with plasmonic and metamaterial coatings, Phys. Rev. E **72**, 016623 (2005)
20. B. Edwards, A. Alu, M.G. Silveirinha, N. Engheta, Experimental verification of plasmonic cloaking at microwave frequencies with metamaterials, Phys. Rev. Lett. **103**, 153901 (2009)
21. A. Alu, N. Engheta, Multifrequency optical invisibility cloak with layered plasmonic shells, Phys. Rev. Lett. **100**, 113901 (2008)
22. E.E. Narimanov, A.V. Kildishev, Optical black hole: broadband omnidirectional light absorber, Appl. Phys. Lett. **95**, 041106 (2009)
23. Q. Cheng, T.J. Cui, W.X. Jiang, B.G. Cai, An omnidirectional electromagnetic absorber made of metamaterials, New J. Phys. **12**, 063006 (2010)
24. Y. Yao, R. Shankar, M.A. Kats, Y. Song, J. Kong, F.A. Capasso, Electrically tunable metasurface perfect absorbers for ultrathin mid-infrared optical modulators, Nano Lett. **12**, 6526 (2014)

25. N.I. Landy, S. Sajuyigbe, J.J. Mock, D.R. Smith, W.J. Padilla, Perfect metamaterial absorber, Phys. Rev. Lett. **100**, 207402 (2008)
26. K. Aydin, V.E. Ferry, R.M. Briggs, A. Atwater, Broadband polarization-independent resonant light absorption using ultrathin plasmonic super absorbers, Nat. Commun. **2**, 517 (2011)
27. M.B. Pu, P. Chen, C.T. Wang, Y.Q. Wang, Z.Y. Zhao, C.G. Hu, C. Huang, X.G. Luo, Broadband anomalous relfection based on gradient low-Q meta-surface, AIP Adv. **13**, 052136 (2013)
28. C. Menzel, C. Helgert, C. Rockstuhl, E.B. Kley, A. Tunnermann, T. Pertsch, F. Leferer, Asymmetric transmission of linearly polarized light at optical metamaterials, Phys. Rev. Lett. **104**, 253902 (2010)
29. M. Stolarek, D. Yavorskiy, R. Kotynski, C.J.Z. Rodriguez, J. Lusakowski, T. Szoplik, Asymmetric transmission of THz radiation through a double grating, Opt. Lett. **38**, 839 (2013)
30. L. Wu, Z.Y. Yang, Y.Z. Cheng, M. Zhao, R.Z. Gong, Y. Zheng, J.A. Duan, X.H. Yuan, Gaint asymmetric transmission of circular polarization in layer-by-layer chiral metamaterials, Appl. Phys. Lett. **103**, 021903 (2013)
31. S.X. Yu, G.M. Shi, C. Zhu, Y. Shi, Generating multiple orbital angular momentum vortex beams using a metasurface in radio frequency domain, Appl. Phys. Lett. **108**, 241901 (2016)
32. S.X. Yu, L. Li, G.M. Shi, C. Zhu, X.X. Zhou, Y. Shi, Design, fabrication, and measurement of reflective metasurface for orbital angular momentum vortex wave in radio frequency domain, Appl. Phys. Lett. **108**, 121903 (2016)
33. L. Zhang, S. Liu, L.L. Li, T.J. Cui, Spin-controlled multiple pencil beams and vortex beams with different polarizations generated by Pancharatnam-Berry coding metasurfaces, Appl. Mater. Interfaces **9**, 36447 (2017)
34. X.B. Yin, Z.L. Ye, J. Rho, Y. Wang, X. Zhang, Photonic spin hall effect at metasurfaces, Science **339**, 1405 (2013)
35. H.Y. Chen, J.F. Wang, H. Ma, S.B. Qu, Z. Xu, A.X. Zhang, M.B. Yan, Y.F. Li, Ultra-wideband polarization conversion metasurfaces based on multiple plasmon resonances, J. Appl. Phys. **115**, 154504 (2014)
36. X.M. Fu, J.F. Wang, Y. Fan, M.D. Feng, M.B. Yan, Y.F. Li, H.Y. Chen, J.Q. Zhang, S.B. Qu, Merging bands of polarization convertors by suppressing Fano resonance, Appl. Phys. Lett. **113**, 101901 (2018)
37. X. Gao, X. Han, W.P. Cao, H.O. Li, H.F. Ma, T.J. Cui, Ultrawideband and high-efficiency linear polarization converter based on double V-shaped metasurface, IEEE Trans. Antennas Propag. **63**, 3522 (2015)
38. Y.H. Liu, X.P. Zhap, Perfect absorber metamaterial for designing low-RCS patch antenna, IEEE Trans. Antennas Propag. **13**, 1473 (2014)
39. L. Zhang, X. Wan, S. Liu, J.Y. Yin, Q. Zhang, H.T. Wu, T.J. Cui, Realization of low scattering for a high-gain Fabry-Perot antenna using coding metasurface, IEEE Trans. Antennas Propag. **65**, 3374 (2014)
40. W.G. Chen, C.A. Balanis, C.R. Birtcher, Checkerboard EBG surface for wideband radar cross section reduction, IEEE Trans. Antennas Propag. **63**, 2636 (2015)
41. W.B. Pan, C. Huang, P. Chen, X.L. Ma, C.G. Hu, X.G. Luo, A low-RCS and high-gain partially reflecting surface antenna, IEEE Trans. Antennas Propag. **6**, 945 (2014)
42. K. Li, Y. Liu, Y.T. Jia, Y.J. Guo, A circularly polarized high gain antenna with low RCS over a wideband using chessboard polarization conversion metasurfaces, IEEE Trans. Antennas Propag. **65**, 4288 (2017)
43. L.J. Liang, M.G. Wei, X. Yan, D.Q. Wei, D. Liang, J.G. Han, X. Ding, G.Y. Zhang, J.Q. Yao, Broadband and wide-angle RCS reduction using a 2-bit coding ultrathin metasurface at terahertz frequencies, Sci. Rep. **6**, 39252 (2016)
44. X. Liu, J. Gao, L.M. Xu, X.Y. Cao, Y. Zhao, S.J. Li, A coding diffuse metasurface for RCS reduction, IEEE Antennas Wirel. Propag. Lett. **16**, 724 (2016)
45. J.X. Su, Y.Y. Cui, Z.R. Li, Y.Q. Yang, Y.X. Che, H.C. Yin, Metasurface base on uneven layered fractal elements for ultra-wideband RCS reduction, AIP Adv. **8**, 035027 (2018)
46. S. Sai, H. Ma, J.F. Wang, Y.Q. Pang, M.D. Feng, Z. Xu, S.B. Qu, Absorptive coding metasurface for further radar cross section reduction, J. Phys. D: Appl. Phys. **51**, 065603 (2018)
47. D.S. Dong, J. Yang, Q. Cheng, J. Zhao, L.H. Gao, S.J. Ma, S. Liu, H.B. Chen, Q. He, W.W. Liu, Z. Fang, L. Zhou, T.J. Cui, Terahertz broadband low-reflection metasurface by controlling phase distributions, Adv. Opt. Mater. **3**, 1405 (2015)
48. S.J. Li, X.Y. Cao, L.M. Xu, L.J. Zhou, H.H. Yang, J.F. Han, Z. Zhang, D. Zhang, X. Liu, C. Zhang, Y.J. Zheng, Y. Zhao, Ultra-broadband reflective metamaterial with RCS reduction based on polarization convertor, information entropy theory and genetic optimization algorithm, Sci. Rep. **5**, 37409 (2016)
49. J.B. Pendry, D. Schurig, D.R. Smith, Controlling electromagnetic fields, Science **312**, 1780 (2006)
50. U. Leonhardt, Optical conformal mapping, Science **312**, 5781 (2006)
51. D. Schurig, J.J. Mock, B.J. Justice, S.A. Cummer, J.B. Pendry, A.F. Starr, D.R. Smith, Metamaterial electromagnetic cloak at microwave frequencies, Science **314**, 5801 (2006)
52. W.X. Jiang, J.Y. Chin, Z. Li, Q. Cheng, R.P. Liu, T.J. Cui, Analytical design of conformally invisible cloaks for arbitrarily shaped objects, Phys. Rev. E **77**, 066607 (2008)
53. H. Ma, S.B. Qu, Z. Xu, J.F. Wang, The open cloak, Appl. Phys. Lett. **94**, 103501 (2009)
54. H. Ma, S.B. Qu, Z. Xu, J.Q. Zhang, J.F. Wang, The simplified material parameter equation for elliptical cylinder cloaks, Chin. Phys. B **18**, 1850 (2009)
55. P. Alitalo, F. Bongard, J.-F. Zürcher, J. Mosig, S. Tretyakov, Expermental verification of broadband cloaking using a volumetric cloak composed of periodically stacked cylindrical transmission-line networks, Appl. Phys. Lett. **94**, 1 (2009)
56. S. Tretyakov, P. Alitalo, O. Luukkonen, C. Simovski, Broadband electromagnetic cloaking of long cylindrical objects, Phys. Rev. Lett. **103**, 103905 (2009)
57. Y.F. Li, J.Q. Zhang, S.B. Qu, J.F. Wang, L. Zheng, H. Zhou, Z. Xu, A.X. Zhang, Wide-band circular polarization-keeping reflection mediated by metasurface, Chin. Phys. B **24**, 014202 (2015)
58. X.M. Ding, F. Monticone, K. Zhang, L. Zhang, D.L. Gao, S.N. Burokur, A.D. Lustrac, Q. Wu, C.W. Qiu, A. Alu, Ultrathin Pancharatnam-Berry metasurface with maximal cross-polarization efficiency, Adv. Mater. **27**, 1195 (2014)
59. N.F. Yu, P. Genevet, M.A. Kats, F. Aieta, J.P. Tetienne, F. Capasso, Z. Gaburro, Light propagation with phase discontinuities: generalized laws of reflection and refraction, Science **334**, 6054 (2011)

60. S.L. Sun, Q. He, S.Y. Xiao, Q. Xu, X. Li, L. Zhou, Gradient-index meta-surface as a bridge linking propagating waves and surface waves, Nat. Mater. **11**, 426 (2012)
61. C.D. Giovampaola, N. Engheta, Digital metamaterials, Nat. Mater. **13**, 115 (2014)
62. T. Koschny, M. Kafesaki, E.N. Economou, C.M. Soukoulis, Effective medium theory of left-handed materials, Phys. Rev. Lett. **93**, 107402 (2004)
63. X.J. Zhang, Y. Wu, Effective medium theory for anisotropic metamaterials, Sci. Rep. **5**, 07892 (2015)
64. A. Alu, A. Salandrino, N. Engheta, Negative effective permeability and left-handed materials at optical frequencies, Opt. Express **14**, 1557 (2006)
65. T.J. Cui, M.Q. Qi, X. Wan, J. Zhao, Q. Cheng, Coding metamaterials, digital metamaterials and programmable metamaterials, Light Sci. Appl. **3**, e218 (2014)
66. L.H. Gao, Q. Cheng, J. Yang, S.J. Ma, J. Zhao, S. Liu, H.B. Chen, Q. He, W.X. Jiang, H.F. Ma, Q.Y. Wen, L.J. Liang, B.B. Jin, W.W. Liu, L. Zhou, J.Q. Yao, P.H. Wu, T.J. Cui, Broadband diffusion of terahertz waves by multi-bit coding metasurface, Light Sci. Appl. **4**, e324 (2015)
67. S. Liu, T.J. Cui, Q. Xu, D. Bao, L.L. Du, X. Wan, W.X. Tang, C.M. Ouyang, X.Y. Zhou, H. Yuan, H.F. Ma, W.X. Jiang, J.G. Han, W.L. Zhang, Q. Cheng, Anisotropic coding metamaterials and their powerful manipulation of differently polarized terahertz waves, Light Sci. Appl. **5**, e16076 (2016)
68. X. Yan, L.J. Liang, J. Yang, W.W. Liu, X. Ding, D.G. Xu, Y.T. Zhang, T.J. Cui, J.Q. Yao, Broadband, wide-angle, low scattering terahertz wave by a flexible 2-bit coding metasurface, Opt. Express **23**, 29128 (2015)
69. R.L. Fante, M.T. MCcormack, Reflection properties of the Salisbury screen, IEEE Trans. Antennas Propag. **36**, 1443 (1988)
70. N. Engheta, Thin absorbing screens using metamaterial surfaces, in: IEEE AP-S International Symposium, San Antonio, Texas, June 16–21, 2002
71. D.J. Kern, D.H. Werner, A genetic algorithm approach to the design of ultra-thin electromagnetic band-gap absorbers, Microw. Opt. Technol. Lett. **38**, 61 (2003)
72. H. Mosallaei, K. Sarabandi, A one-layer ultra-thin meta-surface absorber, Soc. Int. Symp. **1b**, 615 (2005)
73. X.Y. Peng, B. Wang, S.M. Lai, D.H. Zhang, J.H. Teng, Ultrathin multi-band planar metamaterial absorber based on standing wave resonances, Opt. Express **20**, 27756 (2012)
74. R. Yahiaoui, J.P. Guillet, F.D. Miollis, P. Mounaix, Ultra-flexible multiband terahertz metamaterial absorber for conformal geometry applications, Opt. Lett. **38**, 4988 (2013)
75. W.R. Zhu, I.D. Rukhlenko, F.J. Xiao, C. He, J.P. Geng, X.L. Liang, M. Premaratne, R. Jin, Multiband coherent perfect absorption in a water-based metasurface, Opt. Express **25**, 15737 (2017)
76. J.F. Wang, S.B. Qu, Z. Xu, H. Ma, X.H. Wang, D.Q. Huang, Y.F. Li, Super-thin cloaks mediated by spoof surface plasmons, Photonics Nanostruct. Fundam. Appl. **10**, 540 (2012)
77. J.F. Wang, S.B. Qu, Z. Xu, H. Ma, C.M. Wang, S. Xia, X.H. Wang, H. Zhou, Grating-coupled waveguide cloaking, Chin. Phys. Lett. **29**, 034101 (2012)
78. J.F. Wang, S.B. Qu, Z. Xu, H. Ma, J.Q. Zhang, Y.H. Li, X.H. Wang, Super-thin cloaks based on microwave networks, IEEE Trans. Antennas Propag. **61**, 2 (2013)
79. Y.F. Li, J.Q. Zhang, S.B. Qu, J.F. Wang, Y.Q. Pang, Z. Xu, A.X. Zhang, Broadband unidirectional cloaks based on flat metasurface focusing lenses, J. Phys. D: Appl. Phys. **48**, 335101 (2015)
80. J.F. Wang, S.B. Qu, H. Ma, Z. Xu, A.X. Zhang, H. Zhou, H.Y. Chen, Y.F. Li, High-efficiency spoof plasmon polariton coupler mediated by gradient metasurfaces, Appl. Phys. Lett. **101**, 201104 (2012)
81. Y.F. Li, J.Q. Zhang, S.B. Qu, J.F. Wang, H.Y. Chen, Z. Xu, A.X. Zhang, Wideband radar cross section reduction using two-dimensional phase gradient metasurface, Appl. Phys. Lett. **104**, 221110 (2014)
82. H.Y. Chen, H. Ma, J.F. Wang, S.B. Qu, Y.F. Li, J. Wang, M.B. Yan, Y.Q. Pang, A wideband deflected reflection based on multiple resonances, Appl. Phys. A **120**, 287 (2015)
83. Y. Fan, S.B. Qu, J.F. Wang, J.Q. Zhang, M.D. Feng, A.X. Zhang, Broadband anomalous reflector based on cross-polarized version phase gradient metasurface, Acta. Phys. Sin. **64**, 184101 (2015)
84. Y.F. Li, J.Q. Zhang, S.B. Qu, J.F. Wang, H.Y. Chen, L. Zheng, Z. Xu, A.X. Zhang, Achieving wideband polarization-independent anomalous reflection for linearly polarized waves with dispersionless phase gradient metasurfaces, J. Phys. D: Appl. Phys. **47**, 425103 (2014)
85. L. Zhang, X.Q. Chen, S. Liu, Q. Zhang, J. Zhao, J.Y. Dai, G.D. Bai, X. Wan, Q. Cheng, G. Castaldi, V. Galdi, T.J. Cui, Space-time-coding digital metasurface, Nat. Commun. **9**, 1 (2018)
86. M. Moccia, S. Liu, R.Y. Wu, G. Castaldi, A. Andreone, T.J. Cui, V. Galdi, Coding metasurfaces for diffuse scattering: scaling laws, bounds, and suboptimal design, Adv. Opt. Mater. **5**, 19 (2017)
87. L. Zhang, R.Y. Wu, G.D. Bai, H.T. Wu, Q. Ma, X.Q. Chen, T.J. Cui, Transmission-reflection-integrated multifunctional coding metasurface for full-space control of electromagnetic waves, Adv. Funct. Mater. **28**, 33 (2018)
88. M. Moccia, C. Koral, G.P. Papari, S. Liu, L. Zhang, R.Y. Wu, G. Castaldi, T.J. Cui, V. Galdi, A. Andreone, Suboptimal coding metasurfaces for terahertz diffuse scattering, Sci. Rep. **8**, 1 (2018)
89. S. Sui, H. Ma, J.F. Wang, Y.Q. Pang, S.B. Qu, Topology optimization design of a lightweight ultra-broadband wide-angle resistance frequency selective surface absorber, J. Phys. D: Appl. Phys. **48**, 215101 (2015)
90. S. Sai, H. Ma, Y.G. Lv, J.F. Wang, Z.Q. Li, J.Q. Zhang, Z. Xu, S.B. Qu, Fast optimization method of designing a wideband metasurface without using the Pancharatnam-Berry phase, Opt. Express **26**, 1443 (2018)
91. Q.Q. Zheng, Y.F. Li, J.Q. Zhang, H. Ma, J.F. Wang, Y.Q. Pang, Y.J. Han, S. Sui, Y. Shen, H.Y. Chen, S.B. Qu, Wideband, wide-angle coding phase gradient metasurfaces based on Pancharatnam-Berry phase, Sci. Rep. **7**, 43543 (2017)
92. M.C. Feng, Y.F. Li, Q.Q. Zheng, J.Q. Zhang, Y.J. Han, J.F. Wang, H.Y. Chen, S. Sai, H. Ma, S.B. Qu, Two-dimensional coding phase gradient metasurface for RCS reduction, J. Phys. D: Appl. Phys. **51**, 375103 (2018)
93. L.K. Sun, H.F. Cheng, Y.J. Zhou, J. Wang, Broadband metamaterial absorber based on coupling resistive frequency selective surface, Opt. Express **20**, 4675 (2012)
94. Y. Shen, Z.B. Pei, Y.Q. Pang, J.F. Wang, A.X. Zhang, S.B. Qu, An extremely wideband and lightweight metamaterial absorber, J. Appl. Lett. **117**, 224503 (2015)

95. Y. Shen, Y.Q. Pang, J.F. Wang, H. Ma, Z.B. Pei, S.B. Qu, Origami-inspired metamaterial absorbers for improving the larger-incident angle absorption, J. Phys. D: Appl. Phys. **48**, 445008 (2015)
96. Y. Fan, J.F. Wang, Y.F. Li, Y.Q. Pang, L. Zheng, J.Y. Xiang, J.Q. Zhang, S.B. Qu, Ultra-thin and -broadband microwave magnetic absorber enhanced by phase gradient metasurface incorporation, J. Phys. D: Appl. Phys. **51**, 215001 (2015)
97. Y.Q. Pang, J.F. Wang, Q. Cheng, S. Xia, X.Y. Zhou, Z. Xu, T.J. Cui, S.B. Qu, Thermally tunable water-substrate broadband metamaterial absorbers, Appl. Phys. Lett. **110**, 104103 (2017)
98. Y.Q. Pang, J.F. Wang, H. Ma, M.D. Feng, Y.F. Li, Z. Xu, S. Xia, S.B. Qu, Spatial k-dispersion engineering of spoof surface plasmon polaritons for customized absorption, Sci. Rep. **6**, 29429 (2016)

Cite this article as: Ya Fan, Jiafu Wang, Xinmin Fu, Yongfeng Li, Yongqiang Pang, Lin Zheng, Mingbao Yan, Jieqiu Zhang, Shaobo Qu, Recent developments of metamaterials/metasurfaces for RCS reduction, EPJ Appl. Metamat. **6**, 15 (2019)